POLISH MARITIME RESEARCH 2(69) 2011 Vol 18; pp. 44-50
10.2478/v10012-011-0011-1

A new method for detection of rolling bearing faults based on the Local Curve Roughness approach

Mehdi Behzad, Prof.
Abbas Rohani Bastami, M. Sc.
Sharif University of Technology

ABSTRACT

Detection of rolling bearing faults by vibration analysis is an important part of condition monitoring programs. In this paper a new method for detection of bearing defects based on a new concept of local surface roughness, is proposed. When a defect in the bearing grows then roughness of the defective surface increases and measurement of the roughness can be a good indicator of the bearing defect. In this paper a method of indirectly measuring surface roughness by using vibration signal is introduced. Several attached examples including both numerically simulated signals and actual experimental data show the effectiveness of the new, easy-to-implement method.

Keywords: rolling bearing; diagnosis; vibration; local curve roughness

INTRODUCTION

Prediction of rolling bearing life has been a big challenge since implementation of the widely used component. Early work of Stribeck and Goodman, based on Hertz stress theory, was not very successful [1]. The most important improvement in bearing life prediction was the Lundberg-Palmgren (L-P) formula based on Weibull theory of strength of materials. The theory assumes probabilistic life for bearings and finds the life with 90% survival chance, L_{10}, based on equivalent load and dynamic capacity of the bearings [1]. The L-P theory created a base to calculate bearing replacement intervals. In spite of widely acceptance of L-P theory by industry, the final answer to this issue was monitoring of the bearing condition instead of a fixed replacement interval.

Vibration monitoring is one of the most successful techniques of the fault detection in the rolling element bearings. There are various literature sources on the bearing fault detection by vibration analysis [2, 3]. The main techniques include using frequency spectrum [4, 5], envelope analysis [6], kurtosis [7-10], shock pulse [11, 12], synchronous averaging [13], wavelet analysis [14-20], higher spectral analysis [21], cyclic spectrum [22] and empirical mode decomposition [23, 24]. Ball pass frequencies are the main symptoms of defective bearing in the frequency spectrum. Ball pass frequencies may be also used to determine a defective part of the bearing. The major difficulty in the detection of the rolling bearing defects is the masking of weak bearing fault signature by more strong background vibration. The ball pass frequencies are usually hidden between larger peaks in the frequency spectrum. Envelope analysis is a powerful technique in detection of ball pass frequencies, but the resonance frequency must be also known. Other techniques have either some limitations or they are too complicated for practical applications.

In this paper a new method for detection of bearing faults is presented. The method called the Local Curve Roughness (LCR) has been introduced first time by the authors [25]. The LCR method uses a quantitative roughness measure as a bearing defect indicator. Effectiveness of the method is demonstrated by using both numerically-simulated and real vibration data.

FAULT SIGNATURE OF ROLLING BEARINGS

Rolling bearings act as a source of noise and vibration in the machinery. Radially loaded bearings, even if they are healthy, generate vibrations due to a phenomenon called varying compliance [26]. This results from using finite number of rolling elements and change in effective stiffness of the bearing. Presence of a local defect in contact surfaces causes a significant increase in vibration level of the bearing. Local defects including crack, pit and spall in the bearing parts are known to produce a train of impacts which propagate through the bearing and housing to the vibration transducer which is located on the bearing housing. The train of short - duration impulses excites structural resonance and produces a train of

damped natural vibrations [27]. Thus the vibration signature of a faulty bearing can be expressed as [22]:

$$x(t) = \sum_{i=-\infty}^{\infty} q(t) \cdot h(t - iT) \tag{1}$$

where:
the index i denotes i^{th} impact,
h – the impulse response of the structure,
T – the time interval between impacts,
q(t) – periodic function synchronized with shaft rotation, which account for load variation due to bearing defect.

If the defect is located on a fixed part of the bearing then q(t) has a constant value. In a simple model, as follows from [28], h(t) can be considered the impulse response of a single DOF system and characterized by two parameters, namely the natural frequency ω_n and the damping ratio ζ:

$$h(t) = \frac{1}{m\omega_d} e^{-\zeta\omega_n t} \sin(\omega_d t) \tag{2}$$

where:
m – mass,
ω_d – damped natural frequency.

To model real conditions in the equation (1) some vibrations related to the shaft rotation, external sources and random noises are to be added. A more complete model of vibration generation in the rolling bearings is introduced in [29].

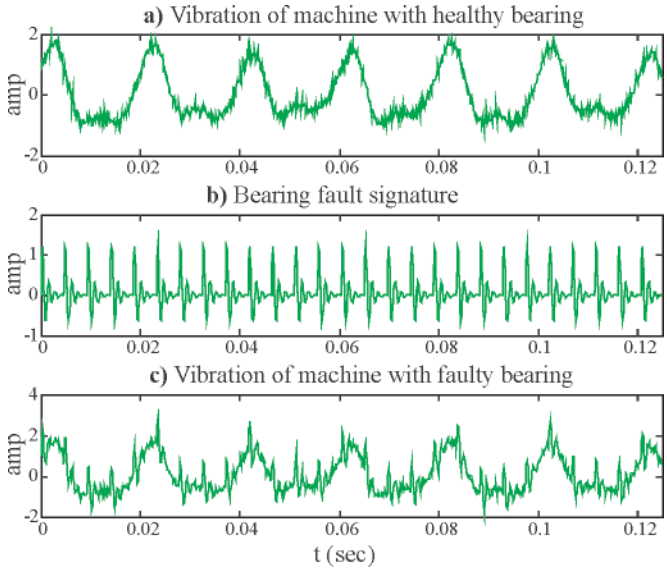

Fig. 1. *Numerically-generated vibration time-waveform curves for:* ***a)*** *a machine with healthy bearing;* ***b)*** *bearing fault signature;* ***c)*** *a machine with faulty bearing, (amp - vibration amplitude, m/s²)*

A numerically- generated vibration signal of a 50 Hz frequency machine with healthy and faulty bearings is shown in Fig. 1. The signal is consisted of the following parts:

1. Vibration due to shaft rotation including the shaft speeds of the first, second and third order with the amplitudes of 1, 0.5 and 0.1 m/s², respectively.
2. Vibration resulting from an external source with the frequency of 37 Hz and amplitude of 0.2 m/s²
3. Vibration due to outer race defect with the ball pass frequency of 4.29x50 = 214.5 Hz , natural frequency of 800 Hz, ζ=0.1 and amplitude of 1.2 m/s²
4. Gaussian white noise with zero - mean value and standard deviation of 0.1 m/s².
5. The frequency spectrum of the signal shown in Fig. 1 is presented in Fig. 2. It is notable that in spite of the high amplitude of bearing fault signature in the time domain, the amplitude of the characteristic frequency in the frequency spectrum is low (of only 0.11 m/s²) and can be easily masked by other vibration sources. The problem arises from using sine bases in Fourier transform to decompose the impulsive vibration of defective bearing. Obviously in the decomposition the first harmonic does not possess the majority of the signal energy and higher harmonics are usually predominant in the spectrum.

To overcome the difficulty, a nonlinear transform is introduced which filters out the harmonic content of the signal and amplifies the train of impulsive vibration. Therefore the Fourier transform of the resultant signal will contain the frequency of impacts and bearing fault signature can be easily detected.

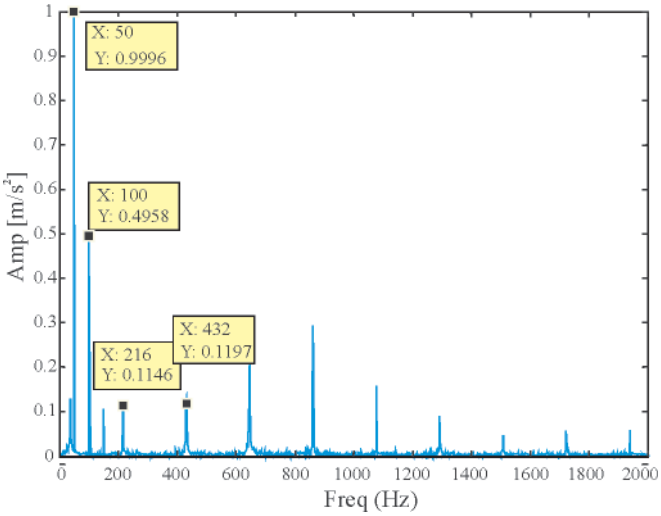

Fig. 2. *Frequency spectrum of the vibration signal shown in Fig (1-c), the graph shows vibration amplitude (m/s²) versus frequency (Hz)*

DEFINITION OF VIBRATION ROUGHNESS

The defective area in the rolling bearing differs, as to the surface roughness property, from the healthy area. In other words, defective area has rougher surface than healthy area. Surface roughness affects the contact force in the rolling process and subsequently changes the generated vibration. The main idea of the proposed method is that rougher surface produces "rougher" vibration [in the sense of a more distinct irregularity of vibration signal]. If one has a quantitative measure of the so understood roughness of vibration signal the defective bearing can be identified. Various parameters may be selected to quantize roughness of a signal. Actually, the vibration roughness shall not only depend on the value of the signal but also on the rate of change of the signal. The definition used herein for the signal roughness x(t) is the actual curve length of the continuous differentiable signal x(t) per unit time, given by:

$$LCR_x(t_0, d) = \frac{1}{d} \int_{t_0}^{t_0+d} \sqrt{1 + \left(\frac{dx}{d\theta}\right)^2}\, dt \tag{3}$$

where:
LCR – stands for local curve roughness,
t_0, d – a moving window position and width, respectively,
x(t) – continuous differentiable signal assumed dimensionless,
θ – the rotation angle equal to θ = Ωt.

If x has a dimension it must be made dimensionless first. If dimension of x is that of acceleration, velocity or displacement, the following dimensionless parameters are proposed:

Acceleration:

$$x^* = \frac{x}{R_m \omega_c^2}$$

Velocity:

$$x^* = \frac{x}{R_m \omega_c}$$

Displacement:

$$x^* = \frac{x}{R_m}$$

where:

- x – used for vibration signal in all three cases of acceleration, velocity and displacement,
- R_m – pitch diameter of the bearing,
- ω_c – cage rotation frequency.

Some properties of the LCR are as follows:

Nonlinearity: It is evident that LCR is a nonlinear transform.

Value of LCR is always greater than one: only the LCR of a constant function x(t) = c equals to 1. LCR of any other signal is greater than one. The LCR can be divided into a constant mean value and oscillating part.

Averaging:

$$d_1 \cdot LCR_x(t_1, d_1) + d_2 \cdot LCR_x(t_1 + d_1, d_2) = (d_1 + d_2) \cdot LCR_x(t_1, d_1 + d_2)$$

FREQUENCY RESPONSE OF LCR

In this section local curve roughness of a sine signal will be studied in more detail. If to assume $x(t) = A\sin(\omega t)$ the LCR will be:

$$LCR_x(t,d) = \frac{1}{d}\int_t^{t+d} \sqrt{1 + (A^*\omega/\Omega)^2 \cos^2 \omega\tau}\, d\tau = \frac{1}{d}\int_t^{t+d} \sqrt{1 + \omega^{*2} \cos^2 \omega\tau}\, d\tau \quad (4)$$

where:

- A^* – non-dimensional amplitude;
- ω^* – non-dimensional frequency defined as $\omega^* = A^*\omega/\Omega$.

To show LCR frequency response the low and high frequencies will be treated separately. For the low frequencies, $\omega^* << 1$, the following approximation can be used:

$$\sqrt{1 + \omega^{*2} \cos^2 \omega\tau} \approx 1 + \frac{\omega^{*2}}{2}\cos^2 \omega\tau \quad (5)$$

Therefore LCR can be approximated by substituting Eq. (5) into Eq. (4):

$$LCR_x(t,d) \approx 1 + \frac{\omega^{*2}}{44} + \frac{\omega^{*2}}{\omega d}\sin(\omega d)\cos(2\omega t + \omega d) \quad (6)$$

Eq. (6) shows that LCR is a combination of a constant value term of $1 + \omega^2/4$ and an oscillating part with a frequency that is twice the original signal frequency. It can be observed that the frequency increasing amplifies both the mean and oscillating part of LCR.

For the high frequency signals of $\omega >> 1$ we use the Fourier series of the integrand of Eq. (4) which is a periodic function of the period π/ω. Since $\sqrt{1 + \omega^{*2} \cos^2 \omega\tau}$ is an even function of τ, only cosine terms remain in the Fourier series which can be written as:

$$\sqrt{1 + \omega^{*2} \cos^2 \omega t} = \frac{a_0}{2} + \sum_{n=1}^{\infty} a_n \cos(2n\omega t)$$

$$a_n = \frac{2\omega}{\pi}\int_0^{\pi/\omega} \sqrt{1 + \omega^{*2}\cos^2 \omega t} \cdot \cos(2n\omega t)dt,\ n = 0,1,2,K \quad (7)$$

The integral in Eq. (7) can be evaluated by using the change of variable $\omega t = \phi$. Then:

$$a_n = \frac{2\omega}{\pi}\int_0^{\pi} \sqrt{\frac{1}{\omega^{*2}} + \cos^2 \phi} \cdot \cos(2n\phi)d\phi,\ n = 0,1,2,K \quad (8)$$

Under the assumption that $\omega >> 1$, the term $1/\omega^{*2}$ can be ignored and we have:

$$a_n \approx \frac{2\omega}{\pi}\int_0^{\pi} |\cos\phi| \cdot \cos(2n\phi)d\phi,\ n = 0,1,2,K \quad (9)$$

The integral in Eq. (9) can be evaluated as follows:

$$a_n = \frac{(-1)^{n+1} 4\omega}{(4n^2 - 1)\pi},\ n = 0,1,2,K \quad (10)$$

From Eq. (10), the first five coefficients of the Fourier series will be:

$a_0/2$	a_1	a_2	a_3	a_4
$2\omega/\pi$	$4/3 \cdot \omega/\pi$	$-4/15 \cdot \omega/\pi$	$4/35 \cdot \omega/\pi$	$-4/63 \cdot \omega/\pi$

By keeping the two first terms of the Fourier series, the LCR of a sine curve will be:

$$\sqrt{1 + \omega^{*2} \cos^2 \omega t} \approx \frac{2\omega^*}{\pi} + \frac{4\omega^*}{3\pi}\cos(2\omega t) \quad (11.a)$$

$$LCR_x(t,d) \approx \frac{1}{d}\int_t^{t+d}\left(\frac{2\omega^*}{\pi} + \frac{4\omega^*}{3\pi}\cos(2\omega t)\right)d\tau \quad (11.b)$$

$$LCR_x(t,d) \approx \frac{2\omega^*}{\pi} + \frac{2\omega^*}{3\pi\omega d}[\sin(2\omega t + 2\omega d) - \sin(2\omega t)] \quad (11.c)$$

$$LCR_x(t,d) \approx \frac{2\omega^*}{\pi} + \frac{4\omega^*}{3\pi\omega d}\sin(\omega d)\cos(2\omega t + \omega d) \quad (11.d)$$

Again the LCR is consisted of two parts: a mean value and an oscillating part with a frequency that is twice the original signal frequency. The increase of ω increases the mean value of the LCR monotonically, but the oscillating part amplitude shows an oscillating trend. The window width has no effect on the mean value but is inversely proportional to the oscillating part.

The actual LCR of a sine curve calculated by using numerical integration of Eq. (4) with low and high frequency approximations, is plotted in Fig. (3-a) and (3-b) where $\Omega = 1$ and $A^* = 1$ are used. The figures verify the low frequency approximation in Eq. (6) and high frequency approximation in Eq. (11-d).

IMPULSE RESPONSE OF CURVE ROUGHNESS

In this section the LCR of the impulse signal x(t) = δ(t) is studied. The impulse with time duration b is defined as follows:

$$\delta(t)=\begin{cases}1/2b\ , & |t|<b\\ 0 & ,\ \text{else}\end{cases} \tag{12}$$

The LCR of impulse function defined by Eq. (12), if d>2b is assumed, is:

$$LCR_{\delta}(t,d)=\begin{cases}1, & t+d<-b\\ 1+1/2bd, & t<-b,\ |t+d|<b\\ 1+1/2bd, & t<-b,\ t+d>b\\ 1+1/2bd, & |t|<b,\ t+d>b\\ 1, & t>b\end{cases} \tag{13}$$

Eq. (13) shows that the impulse width 2b is extended to d + 2b and its height is changed to 1/bd. The increasing of the LCR window length d makes the LCR maximum value decreasing because of the averaging property. Therefore narrow impulses can be amplified by using LCR if only a narrow window will be chosen. LCR of an impulse of b = 0.01 sec calculated by applying a window of the length d = 0.04 sec is shown in Fig. 4.

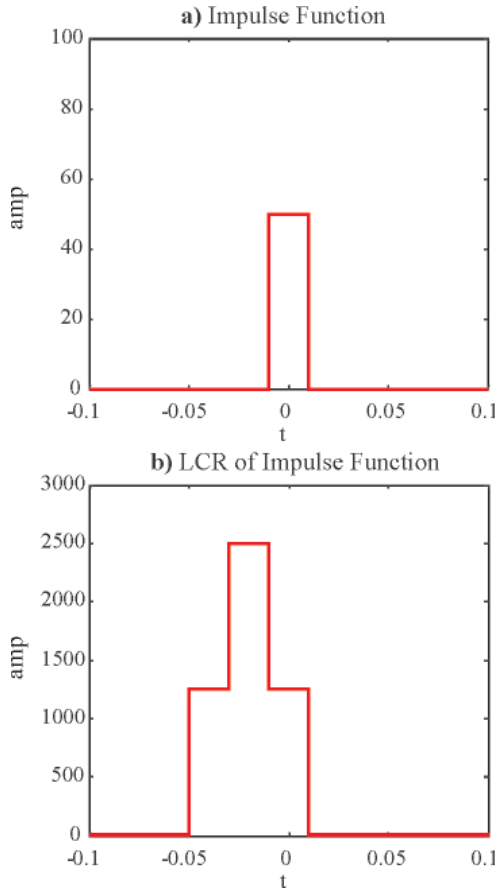

Fig. 4. a) *An impulse of the width b = 0.01 sec,* ***b)*** *LCR of the impulse calculated by applying a window of the length d = 0.04 sec, amplitude (m/s²) versus time (sec)*

DISCRETE LCR

In the case of the discrete signal, x[n], the LCR can be calculated by means of the following formula:

$$LCR_X(n_0,d)=\frac{1}{d}\sum_{i=n_0}^{n_0+d-1}\sqrt{1+\frac{f_s^2}{\Omega^2}[x(i+1)-x(i)]^2} \tag{14}$$

where:
f_s – sampling frequency,
d – window length.

It is necessary to study effect of sampling frequency on the LCR. In Fig. (5) mean value and oscillating part of LCR of a sine curve is plotted against sampling frequency. It is evident that oscillating part is more sensitive to sampling frequency. In order to avoid sampling problems it is necessary to use a sampling frequency at least 20 times greater than the frequency of the signal.

APPLICATION OF LCR TO BEARING FAULT DETECTION

The main idea of LCR for bearing fault detection is that periodic impacts inside the bearing produce local disturbances in the vibration signal, which have large local roughness in terms of its above defined notion. To illustrate this idea, the normal vibration signal of a machine as well as compound normal vibration - bearing fault signature are shown in Fig. (6). LCR decreases the magnitude of oscillating part of harmonic vibration associated with normal shaft vibration, while it amplifies the amplitude of impulsive vibration. This makes LCR an ideal transformation to perceive bearing faults. Since impulsive events are better observed in acceleration signal, its use is more beneficial than that of velocity and displacement.

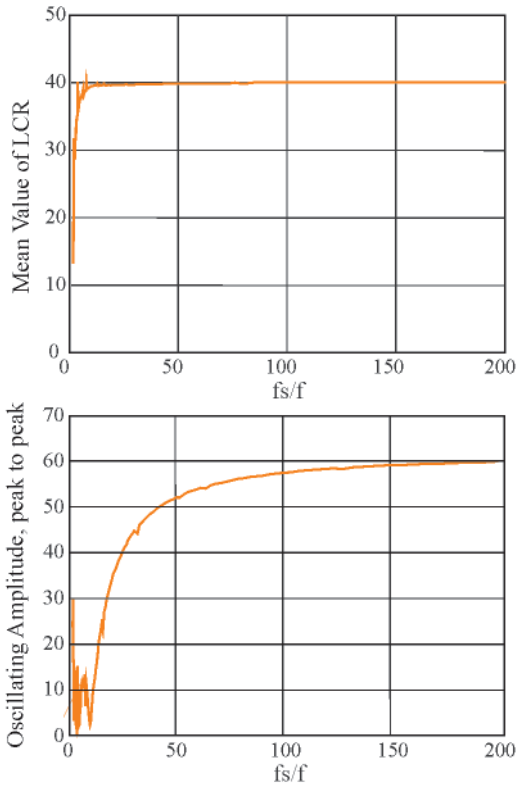

Fig. 5. *Mean value and peak-to-peak amplitude of oscillating part of LCR of a sine curve versus* ***relative*** *sampling frequency (fs/f)*

To interpret the LCR, one should take Fourier Transform of the oscillating part of LCR. The frequency of consecutive impacts will be clear in the resulting spectrum. By comparing this frequency with ball pass frequencies of the bearing, the presence of a defect in the bearing and its location can be recognized as usual.

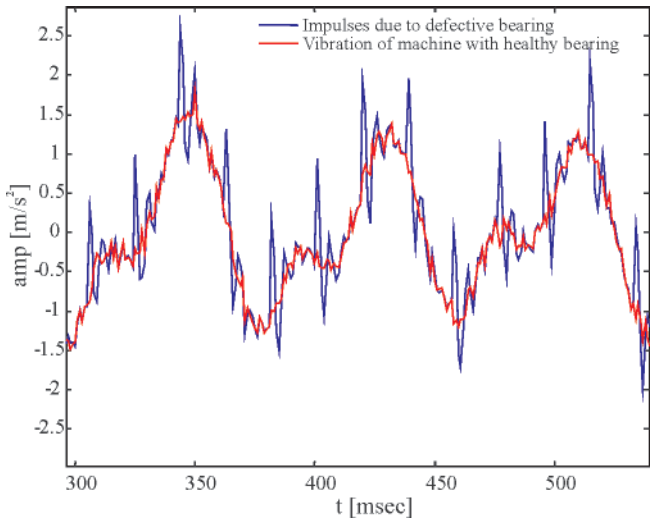

Fig. 6. Comparison of normal vibration signal of a machine and compound normal vibration - bearing fault signature

In the following, several examples will be presented to show the capabilities of the proposed method in diagnostics of rolling bearings. The first two examples deal with numerically simulated signals and the third example presents actual experimental data from a test stand.

Example 1

The vibration signal consists of several components indicated in Tab. (1). The vibration spectrum and LCR spectrum is shown in Fig. (7). While the predominant peak in the vibration spectrum is of 50 Hz frequency, it is totally absent in the LCR spectrum and bearing fault peak is dominant instead. Therefore the bearing fault can be detected in the LCR spectrum, easily and with no confusion.

Tab.1. *Frequency content of vibration signal of example 1*

Component	Amplitude [m/s²]
1st Harmonic: 50 Hz	1
2nd Harmonic: 100 Hz	0.5
3rd Harmonic: 150 Hz	0.1
External Source: 37 Hz	0.2
Bearing outer race frequency: 216 Hz	1.2
Background Gaussian noise	0.1

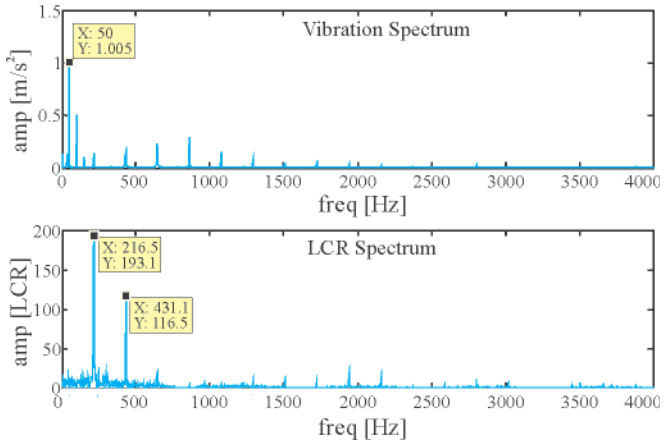

Fig. 7. Vibration and LCR frequency spectrum of vibration signal of example 1(bearing outer race fault)

Example 2

In this example the vibration signal consists of several components indicated in Tab. (2). The vibration spectrum and LCR spectrum are shown in Fig.(8). A twenty - point window is used for computation of LCR. While the predominant peak in the vibration spectrum is of 50 Hz frequency and the bearing fault is not distinguishable, the 50 Hz peak is reduced in the LCR spectrum and the bearing fault peak of 108 Hz frequency is dominant instead. The harmonic vibration of 110 Hz frequency close to the bearing fault frequency is also omitted in the LCR.

Tab. 2. *Frequency content of vibration signal of example 2*

Component	Amplitude [m/s²]
1st Harmonic: 25 Hz	3
2nd Harmonic: 50 Hz	4
External Source: 110 Hz	1
Bearing outer race: 108 Hz	2
Background noise	0.5

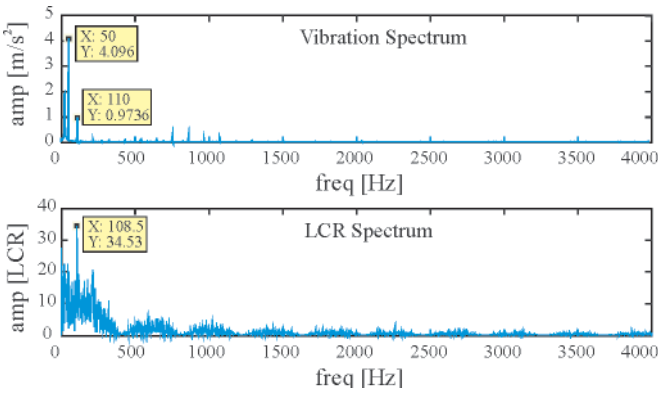

Fig. 8.Comparison of vibration and LCR frequency spectrum of vibration signal of example 2(bearing outer race fault)

Example 3

In this example vibration of a self-aligning ball bearing of 1206 type with an inner race defect is investigated. The test stand is shown in Fig (9). The load is applied to the tested bearing by four screws and measured by a load cell. The shaft is driven by an electrical motor through a variable - speed gear box and belt. The speed can be adjusted in the range from 450 to 4000 rpm. Vibration measurements were made with the use of an Endevco 2235 accelerometer with 20 kHz sampling rate. The inner race defect was introduced artificially by means of EDM[1)].

The shaft speed of 25 Hz and the inner race defect frequency of 206 Hz is applied in this test. The inner race defect produces an amplitude - modulated signal which shows sidebands of rotation speed around harmonics of inner race frequency. The vibration spectrum, envelope spectrum and LCR spectrum is shown in Fig. (10-a) through Fig. (10-c). In the vibration spectrum, 206 Hz frequency response is almost hidden and cannot be detected from the background noise. However the envelope analysis which is a powerful method, reveals the response peak at 206 Hz and sidebands spaced at +/-25 Hz around it and its harmonics. It is notable that the source of the peak at 25 Hz in the envelope spectrum is amplitude modulation

[1)] Electrical Discharge Machining

of bearing fault symptom. The LCR produces a spectrum similar to envelope with a more distinct peak at 206 Hz. This example validates usage of LCR in rolling bearing diagnosis.

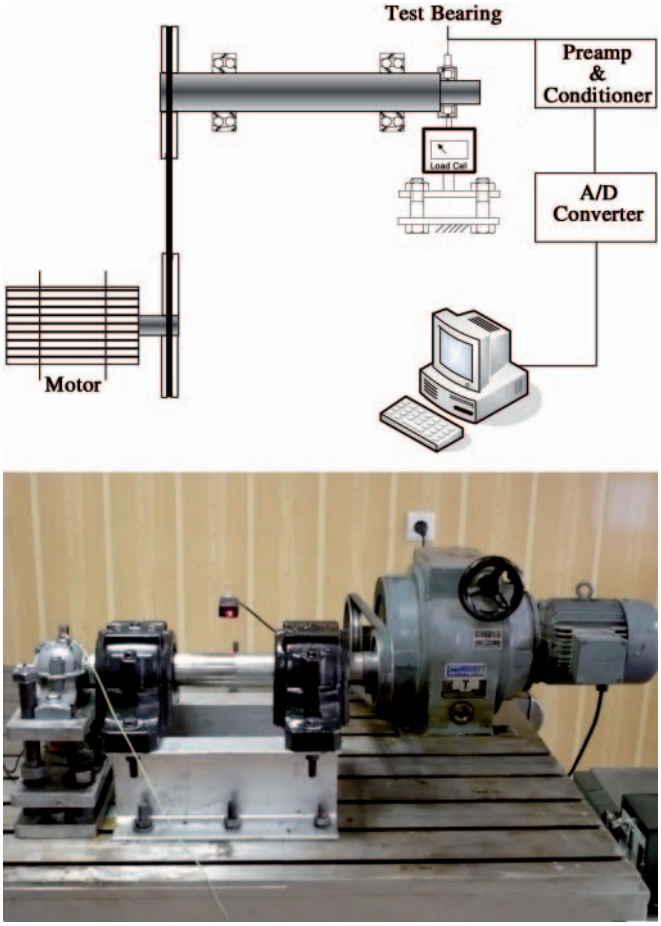

Fig. 9. Experimental test stand for testing the bearings

CONCLUSIONS

In this paper a new method for detection of bearing faults by using vibration analysis is described. The method called Local Curve Roughness (LCR) employs the concept of a curve roughness in a moving window to distinguish between sine waveform and impulsive waveform. The latter one generated by bearing defects is amplified as a result of the above mentioned transformation and this way it can be easily detected in the LCR spectrum. The attached examples showed the advantage of the method as compared with normal vibration spectrum analysis. Several examples given in the paper demonstrated effectiveness of the method. The examples of outer race and inner race fault are included in numerically simulated and actual test data. The simplicity of the proposed method is a key advantage for industrial applications as compared with more advanced techniques for detecting bearing faults.

NOMENCLATURE

b – Impulse width [sec]
d - Window width [sec]
f - Frequency [Hz]
f_s - Sampling frequency [Hz]
h - Impulse response function
LCR - Local Curve Roughness [-]
q - Load [N]
R_m - Bearing pitch radius [m]
t - Time [sec]
T - Time period [sec]
x - Vibration signal
θ - Rotation angle [rad]
ω_c - Cage rotation frequency [rad/sec]
ω_d - Damped natural frequency [rad/sec]
ω_c - Natural frequency [rad/sec]
Ω - Shaft rotation speed [rad/sec]
ζ - Damping ratio [-]

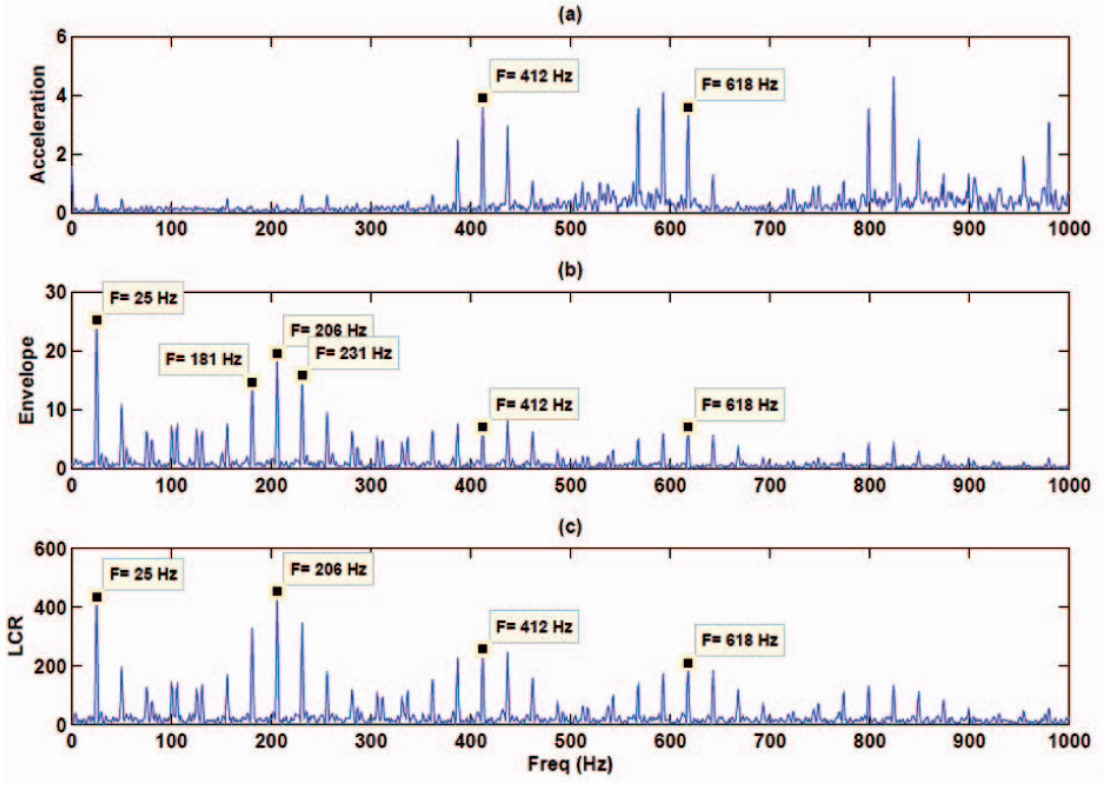

Fig. 10. Comparison of: ***a)*** *Vibration spectrum,* ***b)*** *Envelope spectrum and* ***c)*** *LCR spectrum of vibration signal of example 3 (bearing with inner race fault)*

BIBLIOGRAPHY

1. Zaretski E. V., Poplawski J. V., and Miller C. R.: *Rolling Bearing Life Prediction - Past, Present, and Future*. NASA, NASA/TM-2000-210529, 2000
2. Tandon N. and Choudhury A.: *A review of vibration and acoustic measurement methods for the detection of defects in rolling element bearings*. Tribology International, Vol. 32, No. 32, 1999, pp. 469-480.
3. Tandon N. and Nakra B. C.: *Vibration and acoustic monitoring techniques for the detection of defects in rolling element bearings - a review*. Shock and Vibration Digest, Vol. 24, No. 3, 1992, pp. 3-11.
4. Taylor J. I.: *Identification of bearing defects by spectral analysis*. Trans. ASME, Journal of Mechanical Design, Vol. 102, 1980, pp. 199-204.
5. Berry J. E.: *How to track rolling element bearing health with vibration signature analysis*. S V, Sound and Vibration, Vol. 25, No. 11, 1991, pp. 24-35.
6. McFadden P. D. and Smith J. D.: *Vibration monitoring of rolling element bearings by the high frequency resonance technique-a review*. Tribology International, Vol. 17, No. 1, 1984, pp. 3-10.
7. Dyer D. and Stewart R. M.: *Detection of rolling element bearing damage by statistical vibration analysis*. Trans. ASME, Journal of Mechanical Design, Vol. 100, No. 2, 1978, pp. 229-235.
8. Antoni J.: *The spectral kurtosis: a useful tool for characterizing non-stationary signals*. Mechanical Systems and Signal Processing, Vol. 20, No. 2, 2006, pp. 282-307.
9. Bolaers F., Cousinard O., Marconnet P., and Rasolofondraibe L.: *Advanced detection of rolling bearing spalling from de-noising vibratory signals*. Control Engineering Practice, Vol. 12, No. 2, 2004, pp. 181-190.
10. Dron J. P., Bolaers F., and Rasolofondraibe L.: *Improvement of the sensitivity of the scalar indicators (crest factor, kurtosis) using a de-noising method by spectral subtraction: application to the detection of defects in ball bearings*. Journal of Sound and Vibration, Vol. 270, No. 1-2, 2004, pp. 61-73.
11. *The shock pulse method for determining the condition of antifriction bearings*. SPM Instruments AB, 1980
12. Butler D. E.: *The shock pulse method for the detection of damaged rolling bearings*. NDT International, Vol. 6, No. 2, 1973, pp. 92-95.
13. McFadden P. D. and Toozhy M. M.: *Application of synchronous averaging to vibration monitoring of rolling element bearings*. Mechanical Systems and Signal Processing, Vol. 14, No. 6, 2000, pp. 891-906.
14. Junsheng C., Dejie Y., and Yu Y.: *Application of an impulse response wavelet to fault diagnosis of rolling bearings*. Mechanical Systems and Signal Processing, Vol. 21, 2007, pp. 920-929.
15. Li C. J. and Ma J.: *Wavelet Decomposition of Vibrations for Detection of Bearing-Localized Defects*. NDT & E International, Vol. 30, 1997, pp. 143-149.
16. Mori K., Kasashima N., Yoshika T., and Ueno Y.: *Prediction of Spalling on Ball Bearing by Applying the Discrete Wavelet Transform to Vibration Signals*. Wear, Vol. 195, 1996, pp. 162-168.
17. Ocak H., Loparo K. A., and Discenzo F. M.: *Online tracking of bearing wear using wavelet packet decomposition and probabilistic modeling: A method for bearing prognostics*. Journal of Sound and Vibration, Vol. 302, 2007, pp. 951-961.
18. Purushotham V., Narayanan S., Suryanarayana and Prasad A. N.: *Multi-fault diagnosis of rolling bearing elements using wavelet analysis and hidden Markov model based fault recognition*. NDT & E International, Vol. 38, 2005, pp. 654-664.
19. Rubini R. and Meneghetti U.: *Application of the Envelope and Wavelet Transform Analyses for the Diagnosis of Incipient Faults in Ball Bearings*. Mechanical Systems and Signal Processing, Vol. 15, No. 2, 2001, pp. 287-302.
20. Tse P. W., Peng Y. H., and Yam R.: *Wavelet Analysis and Envelope Detection For Rolling Element Bearing Fault Diagnosis - Their Effectiveness and Flexibilities*. Trans ASME, Journal of Vibration and Acoustics, Vol. 123, 2001, pp. 303-310.
21. Yang D. M., Stronach A. F., and McConnel P.: *Third-Order Spectral Techniques for Diagnosis of Motor Bearing Condition Using Artificial Neural Networks. Mechanical Systems and Signal Processing*, Vol. 16, No. 2-3, 2002, pp. 391-411.
22. Antoni J.: *Cyclic spectral analysis of rolling-element bearing signals: Facts and fictions*. Journal of Sound and Vibration, Vol. 304, 2007, pp. 497-529.
23. Du Q. and Yang S: *Application of the EMD method in the vibration analysis of ball bearings*. Mechanical Systems and Signal Processing, Vol. 21, No. 6, 2007, pp. 2634-2644.
24. Junsheng C., Dejie Y., and Yu Y.: *A fault diagnosis approach for roller bearings based on EMD method and AR model*. Mechanical Systems and Signal Processing, Vol. 20, No. 2, 2006, pp. 350-362.
25. Behzad M., Bastami A.R.: *Concept of Roughness of Vibration in Rolling Bearings Diagnosis*. Proceedings of ISMA Conference, Lueven, 2008
26. Sunnersjo C. S.: *Varying compliance vibrations of rolling bearings*. Journal of Sound and Vibration, Vol. 58, No. 3, 1978, pp. 363-373.
27. McFadden P. D. and Smith J. D.: *Model for the vibration produced by a single point defect in a rolling element bearing*. Journal of Sound and Vibration, Vol. 96, No. 1, 1984, pp. 69-82.
28. C. M. Harris and A. G. Piersol: *Shock and Vibration Handbook*. McGraw-Hill, 5th Ed. 2002
29. M. Behzad, A. R. Bastami, D. Mba: *A New Model for Estimating Vibrations Generated in the Defective Rolling Element Bearings*, ASME Journal of vib & Acoustics,Vol. 133, Aug 2011, pp. 041011-1 to 8

CONTACT WITH THE AUTHORS

Mehdi Behzad, Prof.
Abbas Rohani Bastami, M. Sc.
Mechanical Engineering Department,
Sharif University of Technology
11155-9567, Azadi Avenue,
Tehran, IRAN
email: m_behzad@sharif.edu